Brownian Motion of Vacancy Islands on Ag(111)

Karina Morgenstern,[1] Georg Rosenfeld,[1] Bene Poelsema,[2] and George Comsa[1]
[1]*Institut für Grenzflächenforschung und Vakuumphysik, Kernforschungsanlage Jülich G.m.b.H., D-52425 Jülich, Germany*
[2]*Faculteit der Technische Natuurkunde, Universiteit Twente, Postbus 217, 7500AE Enschede, The Netherlands*
(Received 15 November 1994)

The motion of monatomic deep vacancy islands on crystal surfaces is studied both theoretically and experimentally. We develop a new theoretical model which allows us to deduce the microscopic mechanism of mass transport from measuring the diffusion coefficients of the vacancy islands as a function of their size. This model is applied to experimental results obtained with a fast scanning tunneling microscope on Ag(111) at room temperature. The observed scaling is consistent with a mechanism where the microscopic mass transport is dominated by diffusion of adatoms across the vacancy island rather than along the island boundary.

PACS numbers: 68.35.Fx, 05.40.+j

Steps on crystal surfaces play an important role in many surface processes. With recent advances in direct imaging techniques it is now possible to study their structure and dynamics in atomic detail. In particular, a statistical analysis of thermal step fluctuations was shown to yield information on the microscopic mechanism of the mass transport at steps [1]. In this Letter we show that, as a result of such step fluctuations, two-dimensional vacancy islands perform a random walk across the surface. We derive a formalism that allows one to distinguish different mechanisms of mass transport by measuring the mean square displacement of the center of mass of the vacancy islands as a function of their size. We apply this approach to scanning tunneling microscopy (STM) results on vacancy island motion on Ag(111).

Two-dimensional vacancy islands are the inverse of two-dimensional adatom islands. They are created by removing atoms from the substrate layer, so that monolayer deep depression areas are formed. The boundary of such an inverse island is a single step of monatomic height that forms a closed loop. Thermal fluctuations of this single step, i.e., the transport of material from one part of the step by adatom migration to another one, lead to a motion of the center of mass of the vacancy island. Hence, in this special case, random step fluctuations manifest themselves in a random walk of vacancy islands as a whole across the surface. The same is true for adatom islands. However, adatoms evaporated from the step edge bordering an adatom island are lost by attachment to other step edges somewhere on the surface, whereas for vacancy islands the adatoms are captured inside the vacancy island, so that the island area is conserved. Before discussing an experimental example for this random motion, we establish a relation between the effective diffusion coefficient of a vacancy island and the microscopic mechanisms of mass transport which cause the motion of the vacancy island as a whole.

We consider an equilibrium fluctuation that, within the time t, has moved a vacancy island of diameter d the distance δx to the right (see Fig. 1). Following the line of thought of Pimpinelli *et al.* [2], we consider the individual atomic events causing the change in position as independent from each other. Hence, we equate the net number of atoms that has been moved, $d\delta x n_s$, to the square root of the number of atoms $N(t)$ that have traveled to and from different parts of the step during time t (n_s is the atom density of the surface layer):

$$d\delta x n_s = \sqrt{N(t)}. \tag{1}$$

To find an expression for $N(t)$, we concentrate on two extreme cases. In case (a) the mass transport takes place via diffusion of step adatoms along the vacancy island edge and in case (b) via evaporation of atoms from the step edge and their accommodation at a different part of the step after diffusion over the terrace (Fig. 1). In addition to these two processes, the island motion could also be due to mass transport between vacancy islands by evaporation and diffusion of single vacancies. However, because of the substantial lower diffusivities

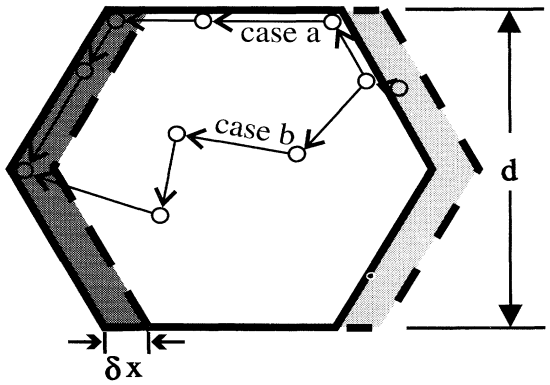

FIG. 1. A vacancy island of diameter d moves δx to the right. The lightly shaded region denotes the material of area $\delta x d$ to be moved into the heavily shaded one. As indicated, two different types of adatom motion can cause the macroscopic motion of the vacancy island.

 0031-9007/95/74(11)/2058(4)$06.00

of single vacancies as compared to adatoms on Ag(111) at room temperature and the higher creation energy of single vacancies, this contribution is unlikely to play a significant role here [3]. For $N(t)$, we can write $N(t) = N_0 t/\tau$, where N_0 is the number of particles on their way from one part of the step to another at a given time, and τ is the average travel time of a particle. Further, $N_0 \propto \rho_{st} d$ [case (a)] and $N_0 \propto \rho_s d^2$ [case (b)], where ρ_{st} and ρ_s denote the equilibrium densities for step adatoms and surface adatoms, respectively. τ is given by $\tau \propto d^2/D_{st}$ [case (a)] or $\tau \propto d^2/D_s$ [case (b)], where D_{st} and D_s are the diffusion coefficients for particle diffusion along the step and across the terrace, respectively. Hence,

$$N(t) \propto D_{st}\rho_{st} t/d\,, \tag{2a}$$

$$N(t) \propto D_s \rho_s t \tag{2b}$$

in case (a) and in case (b), respectively. Combining Eqs. (1) and (2), the final results are

$$\delta x^2 \propto \frac{D_{st}\rho_{st}}{d^3}\, t \tag{3a}$$

and

$$\delta x^2 \propto \frac{D_s \rho_s}{d^2}\, t\,. \tag{3b}$$

Identifying δx^2 with the mean square displacement $\langle(\Delta x)^2\rangle$ obtained from statistical measurements, and defining the diffusion coefficient D of the vacancy island via the Einstein relation $\langle(\Delta x)^2\rangle = 2Dt$, we see that Eqs. (3) describe the vacancy island movement as a random walk and that the corresponding diffusion coefficient scales with the vacancy island size as $D \sim 1/d^3$ for diffusion along the step edge [case (a)] and as $D \sim 1/d^2$ for diffusion over the terrace [case (b)]. The measurement of D for vacancy islands of different diameter d will therefore allow us to distinguish between the two mechanisms of mass transport.

Vacancy island motion has been seen before by STM on Au(111) in an electrochemical cell [4] and on a Co covered Cu(111) surface [5]. In the latter study no movement was observable on the clean Cu(111) surface. On the Ag(111) surface we observed, for the first time, vacancy island motion for a pure system under UHV conditions. Further, we found a mobility already high enough at room temperature to observe a motion of vacancy islands on a time scale of minutes or even seconds (depending on their size). This allowed us to make reliable statistical measurements.

The measurements reported here were done in an UHV system (base pressure below 1.5×10^{-10} Torr) with a beetle-type STM [6]. After preparing an atomically flat and clean Ag(111) surface by sputtering and heating, monolayer deep vacancy islands with diameters between 10 and 75 atoms (= 3,...,22 nm) were produced by an additional short (1–5 sec, depending on the required size) sputtering pulse of 1 keV Ar^+ ions. Adatom islands also produced during sputtering disappeared rapidly. Their motion and dissolution will be discussed elsewhere [7].

Figure 2(a) is an STM image of a Ag(111) surface showing one atomic layer deep vacancy islands. Rescanning the same spot after 4700 sec gives a picture that differs from the former in the position of the vacancy islands [Fig. 2(b)]. Obviously, the larger the vacancy islands are the less they have moved. Note that the vacancy islands (4) and (5) have met and coalesced into one island [(4) and (5)], conserving the total area. On other movies we have seen vacancy islands coming as close as five atomic spacings to one another and resuming their individual random walks without coalescing. We therefore assume an independent motion for larger distances. Vacancy islands that do not coalesce do not change in size at this low vacancy island density. In taking a series of pictures inbetween the two scans shown, the movement of the vacancy islands has been followed more closely. The movement of the vacancy island (3) is shown in Fig. 2(c). It resembles the well-known phenomenon of a Brownian motion (in the sense that a "macroscopic" statistical movement is caused by not seen smaller entities).

We thus checked quantitatively that the motion of the vacancy islands is indeed a Brownian motion. As in

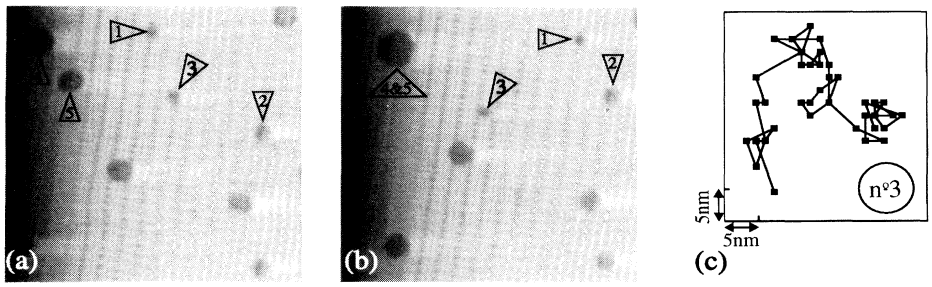

FIG. 2. The scanned region of 173 nm × 173 nm shown in (a) was rescanned after 4700 sec (b). The vacancy islands are 0.24 nm deep (approximately equal to one monatomic step). Inbetween the two shown images, another 46 images were taken at equidistant time intervals $\Delta t = 100$ sec. The 48 monitored positions the vacancy island denoted (3) are shown in (c) enlarged by a factor of 4. Tunneling parameters: $I = 4.9$ nA, $U = 2.9$ V; scanning speed: 13 lines/sec.

field-ion microscopy studies, where adatom migration was investigated first by Ehrlich and Hudda [8], we interpret our data with the help of the random walk formalism first introduced by Einstein [9] and by von Smoluchowski [10]. In order to exclude the effect of any possible drift of the microscope, not the *individual* motion of *one* vacancy island, the *relative* displacement of *two* vacancy islands was measured and analyzed. For the relative displacement distribution of two vacancy islands we expect for a random walk on a two-dimensional lattice

$$W(\bar{r} - \bar{r}_0, t - t_0) = \frac{1}{4\pi(D_1 + D_2)(t - t_0)} e^{-(\bar{r}-\bar{r}_0)^2/4(D_1+D_2)(t-t_0)}, \quad (4)$$

where D_1 and D_2 denote the respective diffusion coefficients of the two vacancy islands. Separated by $\bar{r}_0 = (x_0^{(1)} - x_0^{(2)}, y_0^{(1)} - y_0^{(2)})$ at t_0, their relative position changed during $\Delta t = t - t_0$ to $\bar{r} = (x^{(1)} - x^{(2)}, y^{(1)} - y^{(2)})$.

Projecting the two-dimensional Gaussian distribution (4) onto an arbitrary axis (called x), the expected probability distribution is a one-dimensional Gaussian curve:

$$W'(\Delta x, \Delta t) = \frac{1}{\sqrt{4\pi(D_1 + D_2)\Delta t}} e^{-(\Delta x)^2/4(D_1+D_2)\Delta t}, \quad (5)$$

where $\Delta x = x - x_0$. Equations (4) and (5) differ from a distribution of the displacement of *one* vacancy island just by the replacement of the diffusivity D by the sum of the two diffusivities $D_1 + D_2$. Hence, the Einstein relation derived from Eq. (5) reads

$$\langle(\Delta x)^2\rangle = 2(D_1 + D_2)\Delta t. \quad (6)$$

Before applying these formulas to the experimental data, it is important to realize that, because of the finite imaging time, two vacancy islands [e.g., numbers 1 and 2 in Fig. 2(a)] are scanned at *different* times t_1 and t_2. Assuming an independent motion, this causes no problems as long as $\Delta t_1 = \Delta t_2$, i.e., the time difference between two consecutive scans of the vacancy islands are equal. However, a relative displacement of the vacancy islands results in a small change of Δt, e.g., by moving closer together, Δt for the first scanned vacancy island is larger than for the second one. The effect is at its largest for a displacement perpendicular to the scanning direction. We therefore chose a small enough Δt so that the deviation from a Gaussian curve caused by this time difference can be neglected. With this in mind, we can now analyze the difference of the relative position of two vacancy islands between two consecutive images in a movie.

For the investigation of small and therefore fast moving vacancy islands the STM arrangement had to be modified to meet the above requirement and allow images of 128 lines to be taken every 0.9 sec. Depending on the size of the observed vacancy islands, the time difference between the start of consecutive images was varied between 1 and 100 sec; the time to take one image between 0.9 and 30 sec. For good statistics, movies of up to 640 pictures were taken. Figure 3(a) shows a distribution of a movie of 596 pictures (black bars). The hollow bars in the figure represent a Gaussian distribution of the same number of data points and the same variance. Theoretical and experimental distribution are in good agreement within the statistical error. The same has been done for differently sized vacancy islands and different time scales. Figure 3(b) shows the distribution for another movie of similar vacancy island size and larger Δt. As expected, the curve is broader. From Eq. (6) a proportionality of the mean square displacement $\langle(\Delta x)^2\rangle$ to the time difference Δt is indeed expected and found [e.g., Fig. 3(c)]. The agreement between the theoretical and experimental curves and the linear time dependence leads to the conclusion that the observed motion of the vacancy islands does follow the laws of Brownian motion.

The next question to answer is whether the movement is influenced or even induced by the scanning process. Ebert, Lagally, and Urban [11], for instance, observed a motion of phosphorus vacancies on GaP(110) that was induced by the scanning process. In contrast, it could be shown that the movement here is independent of the scanning process. This was done by varying different scanning parameters as tunneling voltage and

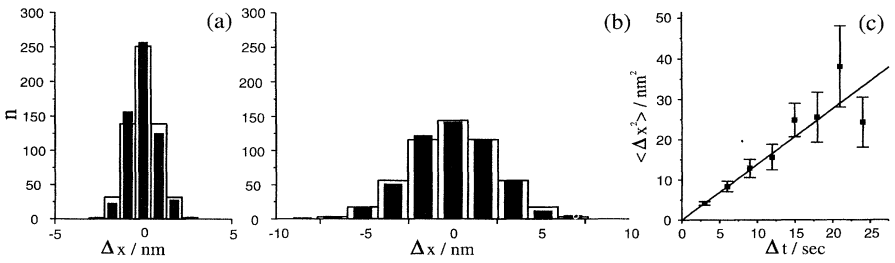

FIG. 3. (a),(b) Distribution of the relative displacement of two vacancy islands of diameters d_1 and d_2 during the time interval Δt. Experimental: black bars; expected Gaussian: hollow bars. (a) $d_1 = 21$ atoms, $d_2 = 24$ atoms, $\Delta t = 1$ sec, total number of analyzed images $n = 596$, and $\langle(\Delta x)^2\rangle = 0.537$ nm^2 [atomic distance on Ag(111) = 0.29 nm]. (b) $d_1 = d_2 = 24$ atoms, $\Delta t = 10$ sec, and $n = 598$ images. (c) Mean square displacement as a function of time; $d_1 = 13$ atoms and $d_2 = 18$ atoms. The least squares fit (straight line) gives $\langle\Delta x^2\rangle/\text{nm}^2 = (1.38 \pm 0.09)\Delta t/\text{sec} - (0.004 \pm 0.501)$.

current, polarization of the tunneling voltage, scanning speed, scanning direction, and number of scans, and by comparing the obtained distributions. For instance, we chose $\Delta t = 240$ sec and a fixed scanning speed less than 15 sec/image. First, we took an image every 240 sec, then we scanned the same spot every 15 sec but only analyzed the images taken every 240 sec. The two distributions are identical within the statistical error. An influence of the scanning on the motion of the vacancy islands would have changed the distributions. If the scanning had even induced the process, the distributions should have differed as much as distributions for $\Delta t = 240$ sec and $\Delta t' = 15$ sec do. This is far beyond the statistical error.

Having established that the vacancy islands indeed perform a Brownian motion independent of the scanning process, we can now analyze the dependence of their diffusivity on their size. We measured the diffusion coefficient of two equally sized vacancy islands for which the common diffusion coefficient $D = D_1 = D_2$ can be obtained from Eq. (6),

$$D = \frac{\langle(\Delta x)^2\rangle}{4\Delta t}. \tag{7}$$

These diffusion coefficients are shown in Fig. 4 versus the diameter d of the vacancy islands. Relating the diffusion coefficient to the diameter by $D \propto d^{\beta}$, the coefficient β can be determined as the slope of a log-log plot (inset of Fig. 3). The resulting slope is $\beta = -1.97 \pm 0.39$. Being very close to 2 we conclude that Eq. (3b) is the relation found here and thus that the underlying process of the movement of vacancy islands is dominated by atoms that evaporate from the step edge onto the enclosed terrace, diffuse over this terrace, and attach at another site of the step. The solid line in Fig. 4 is the, in this case, expected $1/d^2$ curve [12].

Summarizing, we have shown how a statistical analysis of vacancy island motion can be used to determine the microscopic mechanism of mass transport. We measured the diffusion coefficient of vacancy islands on Ag(111) as a function of the island size and found a scaling with the inverse square of the island diameter. This scaling is consistent with a microscopic mass transport dominated by adatoms which evaporate from the island edges onto the terrace and subsequently diffuse across the vacancy island to another part of the island edge [13].

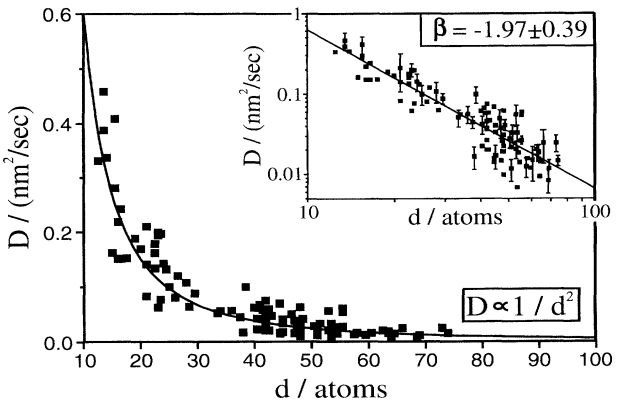

FIG. 4. Diffusion coefficient D as a function of island size. Each data point is calculated from the mean square displacement of at least 80 values. The inset shows the same data as a log-log plot for the determination of the exponent β. Some error bars indicate the statistical error.

We acknowledge stimulating discussions with Ted Einstein and the help of Martin Teske with the modification of the STM electronics.

[1] For example, M. B. Webb, F. K. Men, B. S. Swartzentruber, R. Kariotis, and M. G. Lagally, Surf. Sci. **242**, 23 (1991); M. Poensgen, J. F. Wolf, J. Frohn, M. Giesen, and H. Ibach, Surf. Sci. **274**, 430 (1992); L. Kuipers, M. S. Hoogeman, and J. W. M. Frenken, Phys. Rev. Lett. **71**, 3517 (1993).

[2] A. Pimpinelli, J. Villain, D. E. Wolf, J. J. Métois, J. C. Heyraud, I. Elkinani, and G. Uimin, Surf. Sci. **295**, 143 (1993).

[3] R. C. Nelson, T. L. Einstein, S. V. Khare, and P. J. Rous, Surf. Sci. **295**, 462 (1993).

[4] D. J. Trevor and C. E. D. Chidsey, J. Vac. Sci. Technol. B **9**, 964 (1991).

[5] J. de la Figuera, J. E. Pristo, O. Ocal, and R. Miranda, Solid State Commun. **89**, 815 (1994).

[6] K. H. Besocke, Surf. Sci. **181**, 145 (1987).

[7] K. Morgenstern, G. Rosenfeld, and G. Comsa (to be published).

[8] G. Ehrlich and F. G. Hudda, J. Chem. Phys. **44**, 1039 (1966).

[9] A. Einstein, Ann. Phys. (Leipzig) **17**, 549 (1905); **19**, 371 (1906).

[10] M. von Smoluchowski, Ann. Phys. (Leipzig) **21**, 756 (1906); Phys. Z. **17**, 557 (1916).

[11] Ph. Ebert, M. G. Lagally, and K. Urban, Phys. Rev. Lett. **70**, 1437 (1993).

[12] By measuring the diffusivity at different temperatures, an activation barrier for diffusion of the vacancy islands could be determined. This barrier would correspond to the rate limiting step in the diffusion process, i.e., presumably detachment of kink atoms onto the terrace. Here, we provide a crude estimate for the involved activation barrier in a formal way. For this purpose we define a diffusion frequency by $\nu_D = 4D/l_0^2$, where l_0 is a formal single jump length of the vacancy island corresponding to the motion of one adatom across the vacancy island $l_0 = a_0^2/d$, with $a_0 = 0.289$ nm the lattice constant for Ag(111). Hence, $\nu_D = 4Dd^2/a_0^2$. Using $Dd^2 = 4.9$ nm^4/sec, derived from Fig. 4 and a "usual" prefactor of 10^{12} sec^{-1}, we obtain an activation energy of 0.5 eV. Compared to calculated values for the emission of adatoms from kink sites [3], this is a reasonable result.

[13] Note that the equilibration of the shape of the vacancy islands on Pt(111) at 700 K has been demonstrated to be dominated by the same process [Th. Michely, T. Land, U. Littmark, and G. Comsa, Surf. Sci. **272**, 204 (1992)].

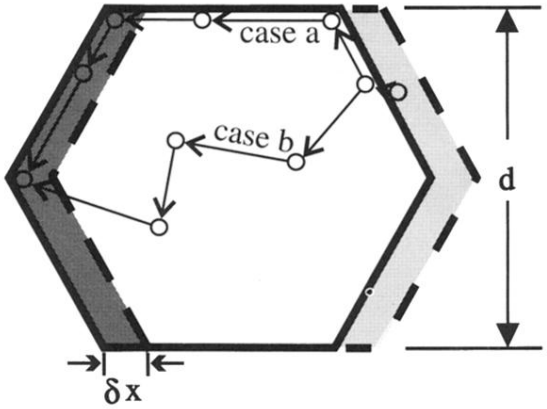

FIG. 1. A vacancy island of diameter d moves δx to the right. The lightly shaded region denotes the material of area $\delta x d$ to be moved into the heavily shaded one. As indicated, two different types of adatom motion can cause the macroscopic motion of the vacancy island.

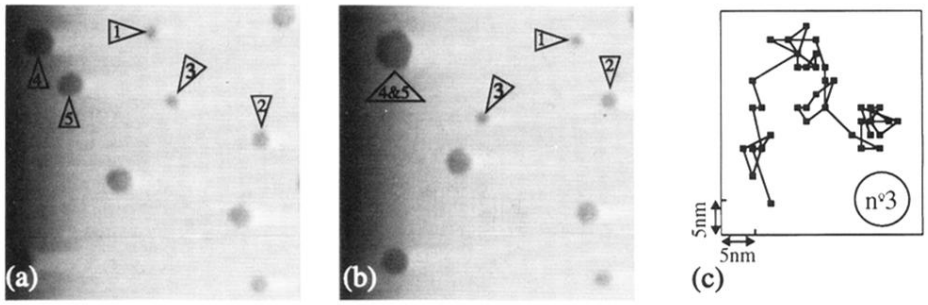

FIG. 2. The scanned region of 173 nm × 173 nm shown in (a) was rescanned after 4700 sec (b). The vacancy islands are 0.24 nm deep (approximately equal to one monatomic step). Inbetween the two shown images, another 46 images were taken at equidistant time intervals $\Delta t = 100$ sec. The 48 monitored positions the vacancy island denoted (3) are shown in (c) enlarged by a factor of 4. Tunneling parameters: $I = 4.9$ nA, $U = 2.9$ V; scanning speed: 13 lines/sec.